Anal. Chem. **2002,** *74,* 6364−6369

Electrochemical Flow Injection Analysis Study of Ion Partitioning at High Surface Area Carbon Fiber Electrodes

Richard S. Kelly,*,† Brian D. Coleman,‡ Tina Huang,‡ Prachak Inkaew,‡ and Theodore Kuwana‡

Department of Chemistry, East Stroudsburg University, East Stroudsburg, Pennsylvania 18301, and Department of Chemistry, University of Kansas, Lawrence, Kansas 66045

Charge-selective electrochemistry was previously shown to occur at high surface area carbon fibers that were produced by fracturing the outer periphery with anodic current or positive potential. The cyclic voltammetric behavior of electroactive species observed at these fibers exhibited a distinct pH dependence related to the protonation/deprotonation of oxygen-containing functional groups at the surface of the carbon fiber. In this paper, electrochemical flow injection analysis (EC-FIA) is used to probe ion partitioning in to and out of the interior microstructure of the treated carbon fiber, for both electroactive and electroinactive species. It was found that the extent of partitioning was the result of both ion charge and hydrated ionic radius, in addition to the level of fracture. It was further observed that the direction of movement for an injected ionic species could be controlled relative to the ion concentration, the pH of the carrier solution, or both. EC-FIA allowed the simultaneous observation of current due to ion movement and that due to electron transfer to a redox-active species. The results presented are consistent with a model in which fixed negatively charged sites in the interior of fractured fibers govern ion partitioning with positively charged ions in the carrier solution, with counterions located in the interior "free" volume.

In a previous paper, a model was developed and computer simulated to explain cyclic voltammetric (CV) responses at ultrahigh surface area carbon fibers (UHSACFs).[1] These high surface area fibers (DuPont E120, 10-μm diameter) were created by the application of a high positive potential or anodic current, during which the double-layer capacitance increased by 2 or 3 orders of magnitude.[2] This capacitance increase was attributed to a concomitant increase in the surface area, as the interior micropores of the fiber became accessible due to "fracture" of the periphery. A major feature of the model, to explain the shape and enhanced size of CV waves, was the entry of electroactive species into the interior volume so that the UHSACF had a component that behaved as a twin-electrode thin-layer cell. Besides the thin-layer element, three other current contributions were considered in the model for computer simulation: the background capacitive current, diffusion of electroactive species to the outer cylindrical-shaped fiber, and adsorption on the carbon surface.

This model was tested with the oxidation of three structurally similar catechols of 3,4-dihydroxyphenethylamine (dopamine), 1,2-dihydroxybenzene (catechol), and 3,4-dihydroxybenzoic acid (DHBA), whose charges span the range of +1 to −1 between pH 2.2 and pH 7.0. The simulation of "best fit" between the computer-generated and experimental CVs gave an internal thin-layer volume that was dependent on the charge of the electroactive species and on the solution pH. For example, DHBA, which has a −1 ionic charge at pH 7.0, gave an internal volume of 0.0, while at pH 2.2, where it is a neutral molecule, the volume increased to 16.5 nL. The thin-layer volume was always less at pH 7.0 than pH 2.2 for these compounds. The pH also affected the charge of the carbon surface, which may be terminated by acidic surface oxides[3−5] and deprotonated to become negatively charged at pH >5. The inhibition of DHBA entering the fiber interior at pH 7.0 can be rationalized by the negatively charged DHBA being excluded by the negatively charged carbon surface. The electrochemistry of ferri-/ferrocyanide is also consistent with this charge repulsion idea whereby the CV waves are attributable primarily to electrolysis at the outer cylindrical surface of UHSAFCs.[1] There are many examples in the literature, particularly dealing with Nafion-coated electrodes, where there is partitioning or rejection of species depending on the charge or size of the species and the solution pH.[6−11] Partitioning into porous microparticles of carbon has also been utilized for liquid chromatographic separations of various species.[12−14]

* Corresponding author. E-mail: rskelly@po-box.esu.edu. Phone: 570-422-3246. Fax: 570-422-3908.

† East Stroudsburg University.

‡ University of Kansas.

(1) Kelly, R. S.; Weiss, D. J.; Chong, S. H.; Kuwana, T. *Anal. Chem.* **1999**, *71*, 413−418.

(2) Weiss, D. J.; Kelly, R. S.; Cumaranatunge, M.; Kuwana, T. *Anal. Chem.* **1999**, *71*, 3712−3720.

(3) McCreery, R. L. In *Electroanalytical Chemistry*; Bard, A. J., Ed.; Marcel Dekker: New York, 1991; Vol. 17, pp 221−374.

(4) Chen, P.; McCreery, R. L. *Anal. Chem.* **1996**, *68*, 3958−3965.

(5) Runnels, P. L.; Joseph, J. D.; Logman, M. J.; Wightman, R. M. *Anal. Chem.* **1999**, *71*, 2782−2789.

(6) Miller, S. A.; Young, V. Y.; Martin, C. R. *J. Am. Chem. Soc.* **2001**, *123*, 12335−12342.

(7) Martin, C. R.; Nishizawa, M.; Jirage, K.; Kang, M. *J. Phys. Chem. B* **2001**, *105*, 1925−1934.

(8) Moschou, E. A.; Chaniotakis, N. A. *Anal. Chem.* **2000**, *72*, 1835−1842.

(9) Bath, B. D.; White, H. S.; Scott, E. R. *Anal. Chem.* **2000**, *72*, 433−442.

10.1021/ac020382m CCC: $22.00
Published on Web 11/07/2002

To examine further the factors governing the partitioning of charged species in to and out of UHSAFCs, electrochemical flow injection analysis (EC-FIA) was undertaken with a variety of simple to structurally more complex charged species. The EC-FIA method is unique for this application since it can determine with high sensitivity the extent of both *capacitive* and *faradaic* currents due to partitioning of charged species in/out of the fiber. The principal factors governing the extent of partitioning in the flowing stream, besides charge, were thought to be size, mobility, and hydrophobicity. This latter effect, important in Nafion, may similarly apply to UHSAFCs. That is, the surface has both distributed fixed charges and noncharged sites.[7,15,16] Another consideration is the applied potential, which determines the electrochemical (double-layer) surface charge, depending on the potential of zero surface charge.[17,18] A decision was made to conduct the ion partitioning experiments at an applied potential that resulted in a "background" current at or close to zero. This minimized or eliminated any faradaic processes due to the electrode itself. For redox species, the applied potential was set at a value where charge transfer would take place, necessitating background current offset.

EXPERIMENTAL SECTION

Reagents and Materials. High-modulus, pitch-based carbon fibers (type E120 from DuPont, Chattanooga, TN) with a nominal diameter of 10−12 μm were used. All chemicals were reagent grade and used as received. Solutions were prepared fresh each day with high-purity water from a Nanopure water system (Barnstead/Thermolyne Corp., Dubuque, IA).

Apparatus. Experiments employed a standard three-electrode system, with potentials referenced to a commercial Ag/AgCl electrode in all measurements. A platinum wire served as the auxiliary electrode in fiber fracture and CV experiments. In flow measurements, a platinum tube at the outlet of the cell served as the auxiliary electrode. Potential control during fracture was accomplished with a Cypress Systems (Lawrence, KS) Omni 90 potentiostat. CV and flow experiments were done using a Cypress Systems Omni 90 (analog), Omni 101 (microprocessor controlled), or CS-1200 (computer controlled) potentiostat. The potential of the working electrode was adjusted so that the observed background current was zero in the presence of carrier solution. This generally resulted in an applied potential between 0 and ±50 mV. Current−time profiles were recorded either on an $X-t$ recorder (Kipp & Zonen model BD41, Bohemia, NY) and digitized using Un-Scan-It software (Silk Scientific, Inc., Orem, UT) or produced in Origin 6.0 (Microcal Software, Cambridge, MA) following data transfer from the Cypress control software. The FIA system consisted of (a) model SX-mini Alitia peristaltic pump (Pump Express, Chicago, IL), (b) pneumatic pulse damper (Cypress Systems), (c) Rainin sample injection valve with 100-μL sample loop, and (d) an in-house-designed flow-by electrochemical cell. Fractured fibers were affixed perpendicular to the flow channel of the cell with a 3-mm length exposed to the solution. The internal volume of the cell was ∼14 μL. The time for the 100-μL sample "plug" to transit the cell was 45−50 s at a flow rate of 0.2 mL/min. The EC-FIA system was mounted onto an electrically grounded 2-in.-thick aluminum sheet with all ac power cables placed in back and below the sheet to minimize electrical noise. The cell was placed in a Faraday cage that had a common ground to the other instruments. Peak currents of ∼50 pA could be resolved at a S/N ratio of unity.

Images of fibers were obtained using a Micrion (Peabody, MA) focused ion beam (FIB) instrument, model 9000.

Fracture Protocol. Ultrahigh surface area carbon fibers were prepared as described previously.[1] In brief, one end of an individual fiber was mounted onto a copper wire with colloidal silver epoxy. Cylindrical electrodes with nominal areas of 0.0031 cm^2 resulted from submerging ∼1 cm of the fiber into an electrochemical cell during fracture. Fibers were subjected to an applied potential of +2.5 V versus Ag/AgCl reference in pH 2.2 phosphate buffer (0.1 M) for times necessary to achieve fracture to the desired level. The distribution of fracture level for each time period was essentially Gaussian, with the observed capacitance value generally falling within ±10% of the mean. After fracture, the electrodes were scanned at 100 mV/s between −200 and +400 mV in the same electrolyte solution until a steady-state voltammogram was observed. The apparent electrode capacitance was calculated from the current envelope, as previously described.[1] This value served as an indicator of the increase in exposed surface area upon fracture. Three levels of fracture were used in this study. Fibers with a capacitance value between 750 and 1500 μF/cm^2 (as normalized to the original unfractured area) are herein referred to as "low fracture", values of 1500−2500 μF/cm^2 as "medium fracture", and values above 2500 μF/cm^2 as "high fracture."

RESULTS AND DISCUSSION

Focused Ion Beam Imaging of Fibers. The topographical features of the fibers as imaged by scanning electron microscopy (SEM), before and after fracture, have been previously described.[19,20] Although both SEM and FIB imaging indicate that fibers are fractured parallel to surface striations, the effects of the fracture on the fiber structure are better illustrated by the FIB images as seen in Figure 1. An end-on view of an untreated, broken fiber is shown in the upper image of Figure 1. The break at the end of the fiber has caused disruption to the surface layer, exposing striated layers below. However, the outer surface above the break shows striations that are essentially intact, without any significant openings or fissures. The FIB image for a fiber fractured to a high level following a clean scalpel cut is seen in the lower image of Figure 1. Extensive damage to the surface is evident in the appearance of open crevices and channels, exposing the interior layers. Additionally, the channels are opened along the laminas extending into the central core. These channels provide a route for ions and molecules, including solvent, to access the nanoporous structure at the interior of the fiber.

(10) Zheng, W.; Maye, M. M.; Leibowitz, F. L.; Zhong, C.-J. *Anal. Chem.* **2000**, *72*, 2190−2199.
(11) Thomsen, K. N.; Baldwin, R. P. *Anal. Chem.* **1989**, *61*, 2594−2598.
(12) Wang, S.; Porter, M. D. *J. Chromatogr., A* **1998**, *828*, 157−166.
(13) Ting, E.-Y.; Porter, M. D. *Anal. Chem.* **1998**, *70*, 94−99.
(14) Ho, M.; Wang, S.; Porter, M. D. *Anal. Chem.* **1998**, *4314*, 4314−4319.
(15) Wang, C. R. C.; Strojek, J. W.; Kuwana, T. *J. Phys. Chem.* **1987**, *91*, 3606−3612.
(16) Aberg, S.; Sharp, M. *J. Electroanal. Chem.* **1998**, *449*, 121−135.
(17) Xu, Y.; Halsall, H. B.; Heineman, W. R. *Electroanalysis* **1992**, *4*, 33−40.
(18) Baldwin, R. P.; Thomsen, K. N. *Talanta* **1991**, *38*, 1−16.
(19) Swain, G. M.; Kuwana, T. *Anal. Chem.* **1991**, *63*, 517−519.
(20) Swain, G. M.; Kuwana, T. *Anal. Chem.* **1992**, *64*, 565−568.

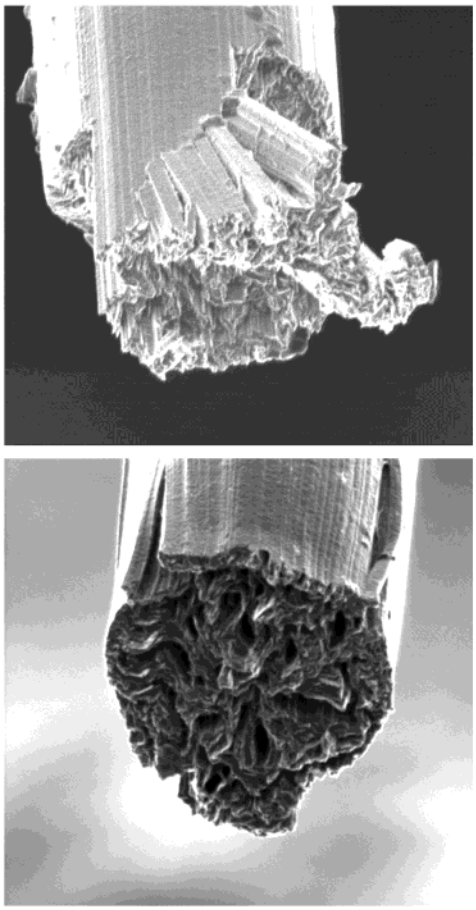

Figure 1. Focused ion beam images of nominal 10-μm carbon fiber. Upper: end-on view of an untreated fiber that was broken by bending the fiber on a flat surface. Lower: end-on view of a treated fiber that was cut with a scalpel prior to fracture (level of fracture >2500 μF/cm^2). The instrument aperture was 25 μm with a field of view of 13−14 μm.

Defining Experiments: Effect of Pure Water and Changing pH. If cations partition from the solution into the interior of the fractured fiber, the entry of positive charge should result in a cathodic current that exactly counterbalances this charge movement. However, the same cathodic current would be observed as the result of an equivalent amount of anionic charge leaving the interior and moving into the surrounding solution. Anodic currents would result from positive charge movement out of the interior or from negative charge movement into the interior.

A description of which charged species flows in or out of the interior of a fractured fiber is less ambiguous in experiments where "pure" water or a different pH solution (compared to background) is injected as the sample. The current response for the first case is shown in Figure 2 where three successive sample plugs of pure water are injected. The background electrolyte solution is 25 mM KNO_3. The sample volume is 100 μL injected at a flow rate of 0.2 mL/min. A current is observed in the anodic direction at a time corresponding to the fractured fiber contacting pure water. At the end of the water plug, the current goes cathodic as the fiber reequilibrates with the 25 mM KNO_3 background solution. Since there is no significant concentration of ions initially in the water, the anodic current must be due to ions flowing from the fiber to the solution phase; i.e., a net flow of K^+ moving from

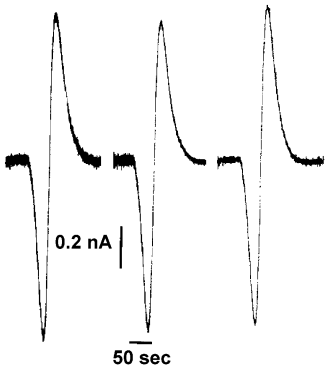

Figure 2. Current versus time response for three successive injections of 100 μL of pure water to a "low fracture" (<1500 μF/cm^2) carbon fiber. Flow rate was 0.2 mL/min. The background solution was 25 mM KNO_3. The initial current direction is anodic.

the fiber to the solution. The cathodic current results from the re-entry of K^+ into the fiber as the fiber returns to its original equilibrium state with the 25 mM KNO_3 background. The equilibrium situation of K^+ and NO_3^- in and out of the fiber is

$$K^+_{(solution)} + NO_3^-{}_{(solution)} \leftrightarrow K^+_{(in)} + NO_3^-{}_{(in)} + (-)_{(in)}$$

where $(-)_{(in)}$ represents the fixed negatively charged sites such as carboxylic acid groups on the surface.[3,4] The $K^+_{(in)} > NO_3^-{}_{(in)}$ since the total $K^+_{(in)}$ is due to the K^+ as counterion to the fixed negative oxygen sites and K^+ in the interior "free" volume. The latter has an equivalent amount of nitrate ion as the counterion. Theoretical treatments of factors governing ion partitioning into charged microstructures have appeared recently.[21−23]

The anodic charge, Q_a, of 8.92 ± 0.64 nC (n = 3) corresponds to 9.2 × 10^{-14} mol of K^+ moving from the fiber to the solution. The length of the fiber exposed in the central channel of the EC-FIA cell is 3 mm. If the entire volume of the 10-μm-diameter fiber is available, the change in the K^+ concentration would be ~0.38 mM. If a conservative estimate of 10% of cylinder volume is used, a concentration change during the event of 3.8 mM is obtained. The cathodic charge, Q_c, is ~30% larger at 12.17 ± 0.31 nC (n = 3), whereas the peak heights differ by ~20% in the opposite direction. The charge difference comes mainly from the trailing edge as the equilibrium of the fiber is being restored with the background KNO_3 solution. Studies with KNO_3 and $NaNO_3$ background solutions have demonstrated that the interior of the fiber becomes saturated with incorporated ions at carrier solution concentrations near 25 mM.

Experiments with pure water are feasible because the reference and auxiliary electrodes are located downstream of the carbon fiber working electrode. Solution conductivity is maintained by ions moving from the fiber to the water, with counterions for these ions moving from the background electrolyte to maintain electroneutrality.

Changes in solution pH give rise to responses as illustrated in Figure 3. Cathodic peaks are observed first for the cases where

(21) Hribar, B.; Vlachy, V.; Bhuiyan, L. B.; Outhwaite, C. W. *J. Phys. Chem. B* **2000**, *104*, 11522−11527.
(22) Vlachy, V. *Langmuir* **2001**, *17*, 399−402.
(23) Mafe, S.; Ramirez, P.; Tanioka, A.; Pellicer, J. *J. Phys. Chem. B* **1997**, *101*, 1851−1856.

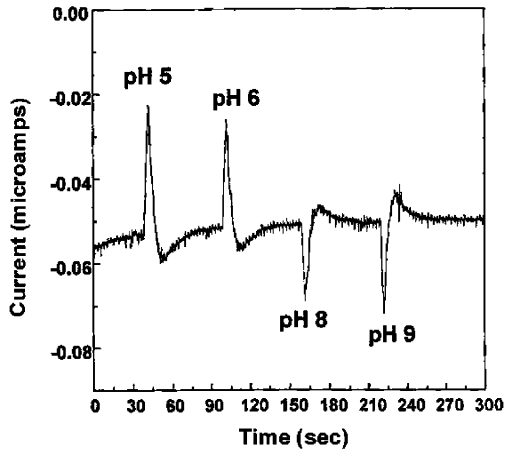

Figure 3. Current response for the injection of pH 5.0, 6.0, 8.0, and 9.0 phosphate buffer solutions (constant ionic strength) to a background of phosphate buffer at pH 7.0.

the injected solution pH is more acidic than the background phosphate buffer of pH 7.0. The most likely explanation for the cathodic direction of these peaks is that protons are moving from the solution into the fiber. When the pH is more alkaline than the pH 7 background, the initial current peaks are in the anodic direction, indicative of protons moving out of, or hydroxide ions going into, the fiber from the solution. The experiment has been repeated with background solutions of differing pH, with the same result. The initial ion movement in each case is characterized by a peak that is sharp and well-defined. However, a return to the previous equilibrium between the background buffer solution (pH 7 in Figure 3) and the fiber is less readily attained, making the current peak in the anodic direction much broader in shape. The reason for this asymmetry is not understood at present. Similar signal profiles have been observed for electroinactive ions at surface-modified electrodes[24−27] and at glassy carbon.[17,28]

EC-FIA Results with Alkali and Alkaline Earth Metal Ions. When alkali or alkaline earth metal ions are injected as samples to a fiber fractured at a high level, the observed responses are characterized by an initial cathodic current indicative of cations from the injected sample entering the interior of the fiber. A smaller, broad anodic peak followed as the sample plug leaves the vicinity of the electrode, indicative of cations exiting the fiber as equilibrium was reestablished with the background KNO_3 solution. Figure 4 shows cathodic peak heights of several injected metal ions plotted versus hydrated size-to-charge ratio. The fiber at which these results were measured was fractured at a high level of ~4000 μF/cm^2. The applied potential was maintained at a constant value of +50 mV. Ba^{2+}, Ca^{2+}, Mg^{2+}, and Li^+ ions (nitrate counterion) lie on a straight line, with Na^+ deviating from linearity. The extent of partitioning into the fiber appears to be correlated to the hydrated size, as normalized to unity charge, for all of the ions. The mean peak currents (n = 3 for each point) were seen to decrease from Na^+ to Li^+ (though not to a significant degree) and similarly, from Ba^{2+} to Mg^{2+}, in accordance with increasing

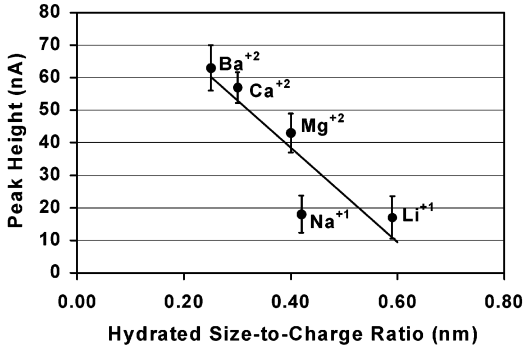

Figure 4. Peak height (nA) versus hydrated size-to-charge ratio (nm) for the injection of alkali and alkaline earth metal ions to a fiber fractured to a high level (near 4000 μF/cm^2). The volume of injected sample was 100 μL at a flow rate of 0.2 mL/min. The applied potential was set at +50 mV for all ions.

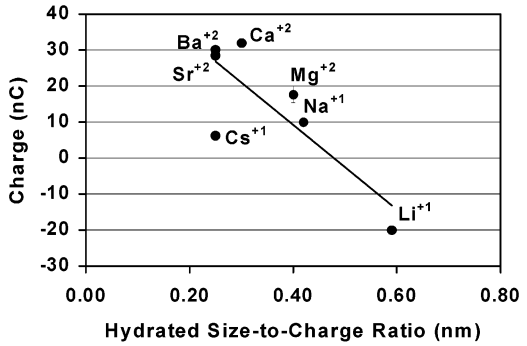

Figure 5. Electrochemical charge (nC) versus hydrated size-to-charge ratio (nm) for alkali and alkaline earth metal ions injected to a fiber fractured at a low level (near 1200 μF/cm^2). The volume of injected sample was 100 μL at a flow rate of 0.2 mL/min. The applied potential was set at −88 mV for all ions. Positive values for charge are cathodic.

hydrated radius. The extrapolated line intersects the zero peak height at ~0.70 nm. More will be said about the significance of this intercept after results at low fracture and varying concentration are presented.

Figure 5 shows representative FIA results for alkali and alkaline earth metals (nitrate counterion) injected at an UHSACF that had been fractured at a low level of ~1200 μF/cm^2. The background solution was again 25 mM KNO_3 with the zero baseline current in this case observed at an applied potential of −88 mV. Each of the injected solutions was 25 mM in nitrate salt. As expected, FIA currents were much less (by nearly 2 orders of magnitude) for fibers at this level of fracture compared to those at high fracture. In the case of $LiNO_3$, the *initial current is anodic*, indicating that Li^+ does not enter the fiber interior. The charge, Q_a, under this anodic peak is added as a negative entry in Figure 5, representing K^+ transfer from the fiber to the solution in a move to attain equilibrium between the two phases. Cathodic current is observed as K^+ re-enters the fiber as equilibrium with the 25 mM KNO_3 background is reestablished. Li^+ at 0.60 nm has the largest hydrated radius of the alkali metals, and lacking the divalent charge of the alkaline earth metals, exclusion by size dominates at low fracture levels.

Concentration Studies with Alkali Metal Cations. Using a 0.5 mM solution of each respective salt as the background solution, the response to sample injection (100 μL) of successively

(24) Ikariyama, Y.; Heineman, W. R. *Anal. Chem.* **1986**, *58*, 1803−1806.
(25) Ye, J.; Baldwin, R. P. *Anal. Chem.* **1988**, *60*, 1982−1984.
(26) Thomsen, K. N.; Baldwin, R. P. *Electroanalysis* **1990**, *2*, 263−271.
(27) Liu, A.; Wang, E. *Anal. Chim. Acta* **1993**, *280*, 223−229.
(28) Nagaoka, T.; Fukunaga, T.; Yoshino, T.; Watanabe, I.; Nakayama, T.; Okazaki, S. *Anal. Chem.* **1988**, *60*, 2766−2769.

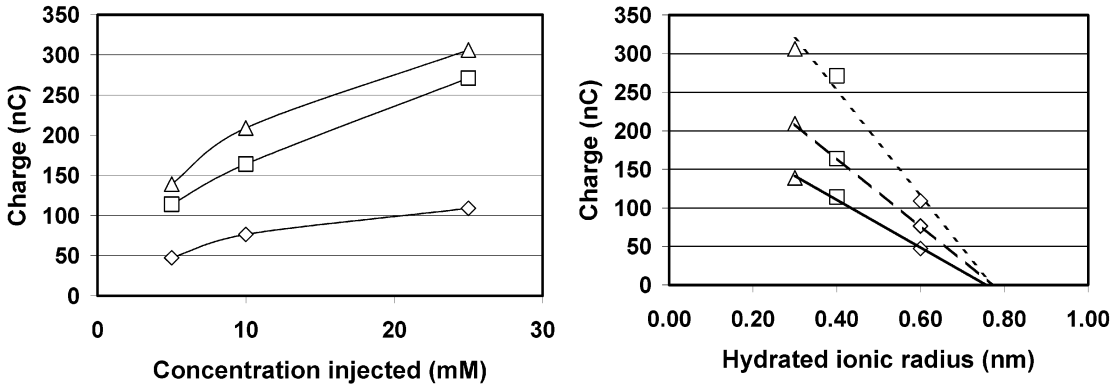

Figure 6. Left side: Graph shows electrochemical charge (nC) as a function of ion concentration (mM) for the injection of $LiNO_3$ (◇), $NaNO_3$ (□), and KNO_3 (△) at concentrations of 5, 10, and 25 mM to a background solution containing 0.5 mM concentrations of each respective salt. Right side: Graph is a replot of the data showing electrochemical charge (nC) for $LiNO_3$ (◇), $NaNO_3$ (□), and KNO_3 (△) as a function of hydrated ionic radius (nm). Concentrations are 5 (−), 10 (- − -), and 25 mM (- - -). The injected sample size is 100 μL at a flow rate of 0.2 mL/min. The fracture level was ∼2400 μF/cm^2.

larger concentrations of $LiNO_3$, $NaNO_3$, and KNO_3 was measured at a fiber fractured to a medium level of ∼2400 μF/cm^2. Figure 6 (left side) shows the observed cathodic charge, Q_c, versus the ion concentration at 5, 10, and 25 mM for these three alkali metal cations. The extent to which the cations partition into the fiber follows the order, $K^+ > Na^+ > Li^+$, which correlates to the order of the increasing hydrated radius, consistent with earlier findings. Figure 6 (right side) shows "best fit" lines for values of the cathodic charge, Q_c, as a function of the hydrated radius for each of these ions. The lines intersect $Q_c = 0$ at ∼0.80 nm. It is interesting to note that the "zero" entry occurs at ∼0.50 nm for fracture at low level (∼1200 μF/cm^2). Although any definitive statement about size limitation to entry based on current data is tenuous, it is nonetheless clear that hydrated ion size and fracture level affect the extent to which ions partition into the interior pores of fractured fibers.

Partitioning of Charged Metal Complexes. It was suggested in previous CV studies of redox species that the sign of the ion charge influenced the extent of entry into the fractured fibers.[1,2] This supposition is supported herein by FIA results for 1 mM concentrations of $K_4Fe(CN)_6$, $K_4Ru(CN)_6$, and $Ru(bpy)_3Cl_2$ in 25 mM KNO_3, injected as 100-μL samples at a flow rate of 0.2 mL/min to a fiber fractured to a medium level. The background solution was also 25 mM KNO_3. The initial current direction is anodic for the *negatively* charged hexacyano metal complexes of iron and ruthenium, as shown in Figure 7, peaks A and B, respectively. Although the current could be due to K^+ moving from fiber to the solution, this movement is not likely since the K^+ concentration (total $K^+ = 29$ mM: 4 mM from the salt of the complex and 25 mM from the KNO_3) in the solution containing complex is higher than that of the background. Thus, the small anodic current (<1 nA) can be attributed to a limited entry of the negative complexes at the periphery of the fractured fiber.

In the case of the *positively* charged bipyridyl complex (Figure 7, peak C), the current is cathodic and 3−5 times larger than those observed for the negatively charged complexes. The applied potential was held between −80 and −100 mV to maintain the background current at or near zero in all of the above cases.

Enhancement of Faradaic Response due to Partitioning. The extent of faradaic current enhancement observed at a fractured fiber above that for an unfractured fiber is illustrated in

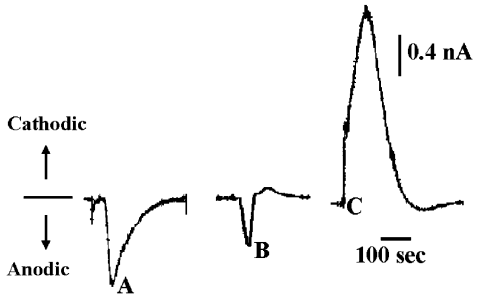

Figure 7. Current responses for the injection of 1.0 mM concentrations of (A) $K_4Fe(CN)_6$, (B) $K_4Ru(CN)_6$, and (C) $Ru(bpy)_3Cl_2$ dissolved in 25 mM KNO_3. The injected sample volume was 100 μL at a flow rate of 0.2 mL/min to a fiber fractured to a medium level. The background carrier solution was 25 mM KNO_3.

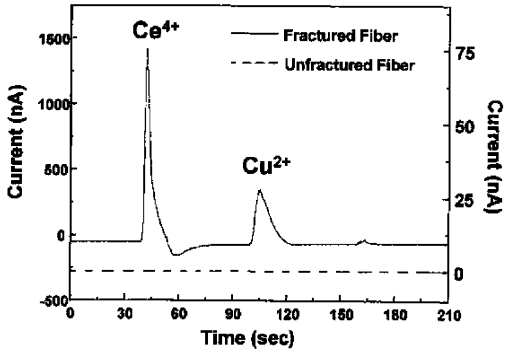

Figure 8. Comparison of response for the reduction of Ce^{4+} and Cu^{2+} ions at an unfractured (- − -) and fractured (−) carbon fiber. Current scale for unfractured fiber (on the right) is 0−75 nA, whereas the current scale for the fractured fiber (on the left) is 0−1500 nA. The fracture level is ∼4000 μF/cm^2.

Figure 8 for the reduction of 1 mM concentrations of Ce^{4+} and Cu^{2+}. The bottom trace in Figure 8 represents the current response of samples injected to an unfractured fiber (current scale of 75 nA), while the top trace illustrates injection to a fiber that had been fractured to a level of ∼4000 μF/cm^2 (current scale of 1500 nA). The sample size in each case was 100 μL at a flow rate of 0.2 mL/min with an applied potential of +50 mV. There is no noticeable current for either of these ionic species at the unfractured fiber, whereas at the highly fractured fiber, current peaks of ∼1500 and ∼750 nA are seen for Ce^{4+} and Cu^{2+}, respectively.

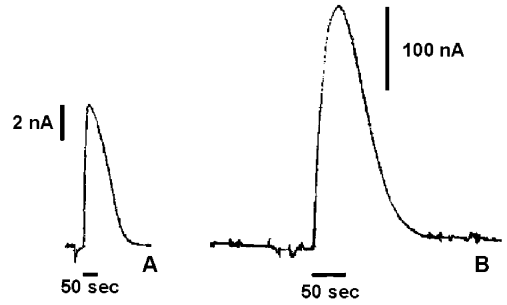

Figure 9. Comparison of faradaic currents as governed by the ion charge for (A) negatively charged $Fe(CN)_6^{3-}$ versus (B) positively charged $Ru(NH_3)_6^{3+}$. The ions at a concentration of 1 mM were dissolved in 25 mM KNO_3. The background carrier solution was 25 mM KNO_3 also. The applied potential was −10 and −500 mV, respectively, for these two ions. The injected sample size was 100 μL at a flow rate of 0.2 mL/min to a fiber at a medium level of fracture. Please note that the given current scales are 2 nA for $Fe(CN)_6^{3-}$ (left) and 100 nA for $Ru(NH_3)_6^{3+}$ (right).

The increase in current is directly attributable to these positively charged ions having access to the interior volume and surface.

Figure 9 illustrates the extent of ion partitioning, as governed by the interior charged sites, by comparing the current response for the injection of negatively charged $Fe(CN)_6^{3-}$ (A, left) to that observed for the positively charged $Ru(NH_3)_6^{3+}$ (B, right). The sample solutions of these complexes were prepared in 25 mM KNO_3, which is also the background solution in these measurements. The applied potentials were −10 and −500 mV for $Fe(CN)_6^{3-}$ and $Ru(NH_3)_6^{3+}$, respectively. These potentials are values at which these ions undergo faradaic reduction. The peak currents were 8 nA for the *negatively* charged ferricyanide and 280 nA for the *positively* charged ruthenium hexamine. Both species undergo one-electron reduction and have similar diffusion coefficient values. Thus, the larger current response for the positively charged ion is attributed to its partitioning into the interior of the fractured fiber in contrast to little or no partitioning for the highly negatively charged ferricyanide. The results show the same charge dependence, as discussed earlier for $Fe(CN)_6^{4-}$ and $Ru(bpy)_3^{2+}$, where the response was due solely to ion partitioning. It is interesting to note that the difference in response for 1 mM ferricyanide at unfractured (2−3 nA) and fractured (3−8 nA) fibers is very small in comparison to the positively charged ruthenium hexamine, where the response increases by a factor of ∼100 upon fiber fracture.

A phenomenon heretofore unobserved is the simultaneous event of ion movement, due to partitioning, and electron transfer (i.e., faradaic current) due to a redox reaction. Thus, if 1 mM $K_3Fe(CN)_6$ is injected as a sample, the response shown in the upper curve of Figure 10 results. The background was 25 mM KNO_3. The applied potential was set near 0 V, a potential at which ferricyanide is reduced to ferrocyanide. The double wave occurs because, in this case, the concentration of K^+ in solution is 3 mM, which is less than the 25 mM in the background at which the fiber was equilibrated. Thus, K^+ in the interior partitions out of the fiber simultaneously with the reduction of ferricyanide to ferrocyanide. This movement of K^+ from the interior of the fiber duplicates closely what is happening when pure water is injected as the sample to a background 25 mM KNO_3 as seen in the lower curve of Figure 10. This curve was taken from one of the water

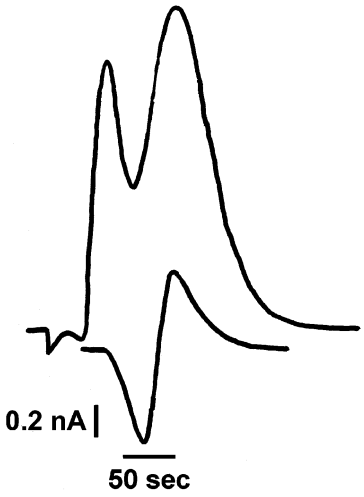

Figure 10. Upper curve: current response when a 100-μL sample of 1 mM $K_3Fe(CN)_6$ is injected to a fiber at a fracture level near 1800 $\mu F/cm^2$. The background carrier solution was 25 mM KNO_3. Lower curve: current response for pure water injection to the 25 mM KNO_3 background (taken from one of the injections shown in Figure 2). The flow rate was 0.2 mL/min for both traces.

injections shown earlier in Figure 2. Of course, when the ferricyanide is dissolved in 25 mM KNO_3 as the sample (Figure 9A), the K^+ concentration in the solution is near that of the background so the current due to K^+ partitioning is small compared to the larger faradaic current peak. The combination of faradaic and ion partitioning response has been checked with $KClO_4$ as the background electrolyte with similar results.

CONCLUSIONS

We have shown that EC-FIA provides high-sensitivity measurement of ion movement in to and out of fractured carbon fibers. The movement or partitioning of ions is proposed to arise from the exposure of interior nanopores and carbon sublayers with negative charge sites affixed to surfaces. Thus, positively charged species are more readily incorporated into the interior than negatively charged ones. The extent of fracture and the ion size are also determining factors. At low levels of fracture, the entry appears to be limited to cations with hydrated radius of less than ∼0.50 nm and, at higher fractures, limited to 0.70−0.80 nm. The effect of fracture to enhance the current for a faradaic process was illustrated by looking at the reduction of Ce^{4+} and Cu^{2+}. The large difference in the current observed for the reduction of $Ru(NH_3)_6^{3+}$ compared to $Fe(CN)_6^{3-}$ further demonstrated the charge selectivity of fractured fibers. To our knowledge, the delineation of a current due to a faradaic reaction and to ion partitioning taking place simultaneously is unique to EC-FIA of fractured fibers.

ACKNOWLEDGMENT

The authors gratefully acknowledge the support provided by NSF Award CHE-9900344 and the University of Kansas Center for Research. The authors thank Dr. Robert Dunn for assistance in obtaining the FIB fiber images. Helpful discussions with Dr. Al Gotch are also acknowledged.

Received for review June 10, 2002. Accepted September 16, 2002.

AC020382M